Angular correlations and widths for alpha-particle decay in the reaction ^{7}Li(^{12}C,^{15}N$^* \rightarrow \alpha+^{11}B_{g.s.}$)$\alpha$

J.A. Liendo
Centro de Fisica, IVIC, Caracas, Venezuela
and Department of Physics, Florida State University, Tallahassee, Florida 32306

N.R. Fletcher, E.E. Towers,* and D.D. Caussyn†
Department of Physics, Florida State University, Tallahassee, Florida 32306
(Received 18 May 1994)

The partial widths for ground-state alpha-particle decay of selected excited states in ^{15}N have been determined by measuring the production cross section and the ground-state alpha-particle decay cross section in the reaction ^{7}Li(^{12}C,^{15}N$^*\rightarrow \alpha+^{11}B_{g.s.}$)$\alpha$ at a bombarding energy of 90 MeV. Decay cross sections are determined by making use of a symmetry property of the decay angular correlation. The method produces agreement within experimental uncertainties for the one state for which a partial width measurement already exists, E_x(^{15}N)=11.44 MeV. Reduced widths for some states place restrictions on J values previously reported.

PACS number(s): 23.60.+e, 25.70.Hi, 27.20.+n

I. INTRODUCTION

The ^{15}N nucleus has been studied extensively experimentally and theoretically [1], however the alpha-particle decay properties of most of its excited states remain unknown. The alpha-particle decay of a few states has been investigated by use of $\alpha+^{11}$B resonance reactions and in some cases a decay branching ratio has been obtained [1,2]. Alpha-particle structure properties of some states in ^{15}N have also been inferred on the basis of strong population of those states in alpha-particle transfer reactions accompanied by weak population of those same states in two-particle and three-particle transfer reactions. Quantitative structure factors from transfer reactions rely on the applicability of the direct reaction model and on the assumption of a pure reaction mechanism, neither of which may be totally realistic.

The objective of the current work is to measure the alpha-particle decay branching fractions for selected states in ^{15}N by use of a method which is independent of beam energy and reaction angle. Knowledge of these branching fractions not only gives direct information about the ($\alpha+^{11}$B) structure of ^{15}N excited states, but also it can be used to check the direct reaction character of the formation mechanisms occurring in reactions which populate the excited states and in that sense it gives alpha-particle cluster information which is independent of direct reaction calculations for cluster transfer. The reaction used is the sequential breakup reaction ^{7}Li(^{12}C,^{15}N$^* \rightarrow \alpha+^{11}$B)$\alpha$, at a ^{12}C bombarding energy of 90 MeV. We obtain double-differential cross sections for the formation and subsequent alpha-particle decay of states in ^{15}N. These reaction plane decay cross sections, usually referred to as angular correlations, are symmetric about 90° in Ψ_Z (see Fig. 1) which is a result consistent with the predominantly diagonal density matrix (PDDM) assumption [3]. This assumption also implies azimuthal isotropy in the correlation which is used to obtain the total decay cross section. The branching fraction is obtained by dividing this result by the corresponding ^{15}N* production cross section measured in a ^{12}C(^{7}Li,α)^{15}N* reaction at the same center of mass reaction angle and energy ($E_{c.m.}$=33.2 MeV). In cases for which the total width of the resonant state is known, we also obtain the alpha-particle partial width, and for specific decay assumptions, the reduced width. A comparison of the extracted reduced widths and the Wigner limits identifies the observation of a known state [2] at 11.436 MeV and limits or eliminates some proposed spin assignments of others.

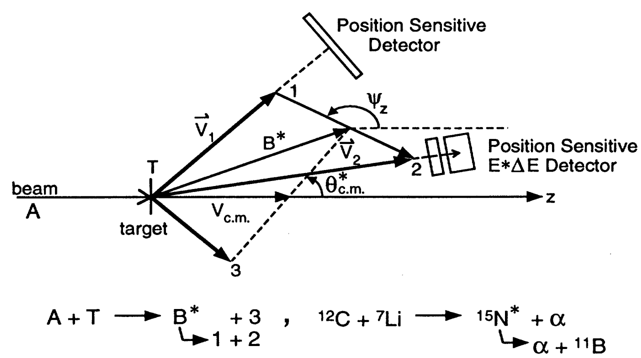

FIG. 1. Schematic of detector arrangement and velocity addition diagram for the coplanar, sequential binary, decay reaction, ^{7}Li(^{12}C,^{15}N$^* \rightarrow \alpha+^{11}$B)$\alpha$.

*Present address: THREE BOND U.S.A., Inc., West Chester, OH 45069.

†Present address: Department of Physics, University of Michigan, Ann Arbor, MI 48109.

II. EXPERIMENTAL METHOD AND PROCEDURE

A sequential breakup reaction, $T(A, B^* \rightarrow 1+2)3$, consists of the formation of an excited nucleus B^*, in a two-body intermediate state, followed by a particle decay of B^* to form the three-body final-state. All three-body final-state reactions which we have investigated proceed sequentially in this manner. A velocity addition diagram for the reaction is shown in Fig. 1, which is also a schematic for the placement of detectors. The method of resonant particle decay spectroscopy (RPDS) which we employ is very similar to the pioneer work of Rae and his co-workers at Oxford [4] and Berkeley [5]. Much of the details of our method are described elsewhere [6] and we will only summarize here.

The kinetic energies, E_1 and E_2, and the angular positions, θ_1 and θ_2, of the decay products, 1 and 2, are measured in position sensitive detectors, and the Z of particle 2 is determined in the $E^*\Delta E$ detector. By assuming the masses of the particles and that only three particles exist in the final state, the reaction is kinematically complete and the energy of particle three can be calculated. From this information one can calculate for each event a Q value given by

$$Q = E_1 + E_2 + E_3 - E_A, \qquad (1)$$

the relative energy between particles 1 and 2, $E_{\rm rel}$, which is the decay energy of B^*, and the angles $\theta^*_{\rm c.m.}$ and Ψ_z which describe the formation and decay of ^{15}N*. Although the $E \times \Delta E$ detector is position sensitive in both the X and Y directions, any meaningful data out of the horizontal reaction plane are unobtainable since the alpha-particle detector (1) produces only horizontal position information.

For the current experiment, a 51 MeV beam of ^{12}C^{+5} ions, produced by the Florida State University S-FN-Tandem accelerator, is stripped to the +6 charge state and injected into the FSU-LINAC where it is accelerated to its final energy of 90 MeV. The beam bombards a ^{7}Li target of areal density ~200 μg/cm^2 where the reaction ^{7}Li(^{12}C,^{15}N$^* \rightarrow \alpha+^{11}$B)$\alpha$ is initiated. Reaction products are detected in coincidence with a resolving time sufficient to identify the event as occurring within one beam pulse from the LINAC. Detector (1) is 1 cm × 5 cm in area with a 0.1 cm thickness and with the horizontal position sensitivity in the longest dimension. The heavy-ion $E \times \Delta E$ detector, (2), is 1 cm in diameter. Detectors (1) and (2) are located on the same side of the beam with their centers 27° and 8° from the beam direction, respectively. A 36-μm aluminum foil is placed in front of detector (1) to stop the prolific yield of elastically scattered beam particles. Although the masses of the detected particles are not determined directly, it becomes obvious from the Q-value spectrum, constructed by use of Eq. (1), that the particles detected in coincidence, assumed to be ^{4}He and ^{11}B, can be unambiguously identified. With the detectors about 10 cm from the target for large detection efficiency, mass identification by time of flight is not possible, since the flight times of all particles with energies of 2 to 10 MeV/nucleon are ~2 to 5 nsec and the time resolution obtained for these detectors is about 15 nsec. Prior to the experiment the detectors are calibrated in position and energy by use of collimating grids and the reaction ^{12}C(^{12}C,α)^{20}Ne* observed at carbon bombarding energies of 25 and 45 MeV. The method of calibration and many other experimental details similar to this experiment have been discussed elsewhere [6,7].

III. RESULTS AND DISCUSSION

A. Spectra for Q-value and decay energies

A spectrum of the negative Q value for events, as calculated by use of Eq. (1), is shown in Fig. 2. Since the energies in Eq. (1) are calculated from the energy signals and the calibration procedures, the dispersion in Fig. 2 is arbitrary, and here it is chosen as 0.1 MeV per channel. The shaded region of the spectrum represents the approximate Q-value gate used to identify those ^{15}N* decay events which result in an alpha particle and ^{11}B$_{\rm g.s.}$. The energy resolution in this ground-state Q-value peak is approximately 2 MeV. In the spectrum (Fig. 2) there are indications of alpha-particle decays to excited states of ^{11}B as indicated in the enclosed scale. Although it appears from Fig. 2 that some events in the gate may have the ^{11}B nucleus left in the first excited state, a scatter plot of $E_{\rm rel}$ vs $-Q$ would show correspondingly different values of $E_{\rm rel}$, i.e., decay energies to ^{11}B*, and no such events are found to occur. The prominent continuum to the right side of the spectrum is undoubtedly composed of background coincidence events for which detector (1) did not record an alpha particle, and of other multiparticle reaction events involving a boron nucleus of different mass.

For each event identified as a ground-state decay in Fig. 2, the center of mass decay angles, $\theta^*_{\rm c.m.}$ and Ψ_z measured in the horizontal reaction plane, are determined for

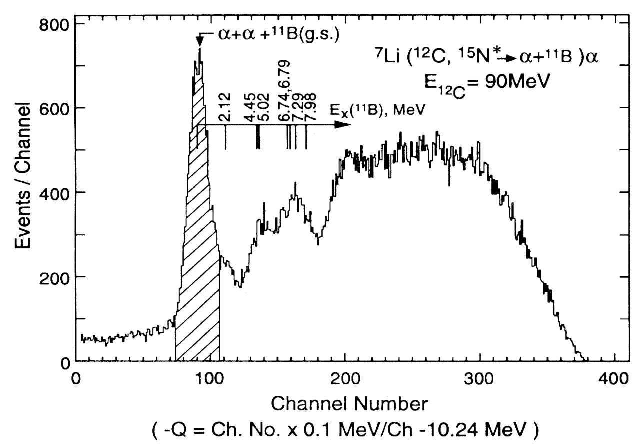

FIG. 2. A spectrum of Q values generated by use of Eq. (1), calculated event by event for the reaction ^{12}C+Li$\rightarrow \alpha+\alpha+^{11}$B.

the two binary decay processes. Also calculated is the decay energy for the second decay, $E_{rel}(\alpha\text{-}^{11}B)$, which is related to the ^{15}N excitation energy by $E_x = E_{rel} + 10.990$ MeV. In the lower portion of Fig. 3 a spectrum of these decay energy values is displayed at a dispersion of 10 keV per channel. The prominent peaks are labeled by the corresponding ^{15}N excitation energies. These are the first reported particle decays of the states at $E_x = 12.55$ and 13.00 MeV. The upper portion of Fig. 3 is a scatter plot of E_{rel} vs Ψ_z for these events. For the six prominent states with $E_x < 14.2$ MeV, decays are observed for a very broad angular range in Ψ_z of approximately 150° for this one placement of detectors. The data set also contains a range in $\theta^*_{c.m.}$ from 30° to 60°, but the range for any particular excitation is more restricted.

Just from the kinematics, the energy resolution in E_{rel} is known to be dependent on the angles $\theta^*_{c.m.}$ and Ψ_z. Many more details in the E_{rel} spectra can be revealed by selecting smaller angular ranges of the angular phase space. Examples of such spectra in the lowest energy region of Fig. 3 are shown in Fig. 4. Here we observe quite clearly the state at 11.29 MeV excitation, only 300 keV above the alpha-particle decay threshold. In Fig. 4(b) we see an example of spectrum fitting in an energy region, which in Fig. 3 appeared to be background and is now revealed to consist of several known excited states of ^{15}N. The excitation energies shown in Fig. 4(b) are the result of the fitting procedure. This is the first reported alpha-particle decay of the states at excitations of 11.29 and 12.35 MeV.

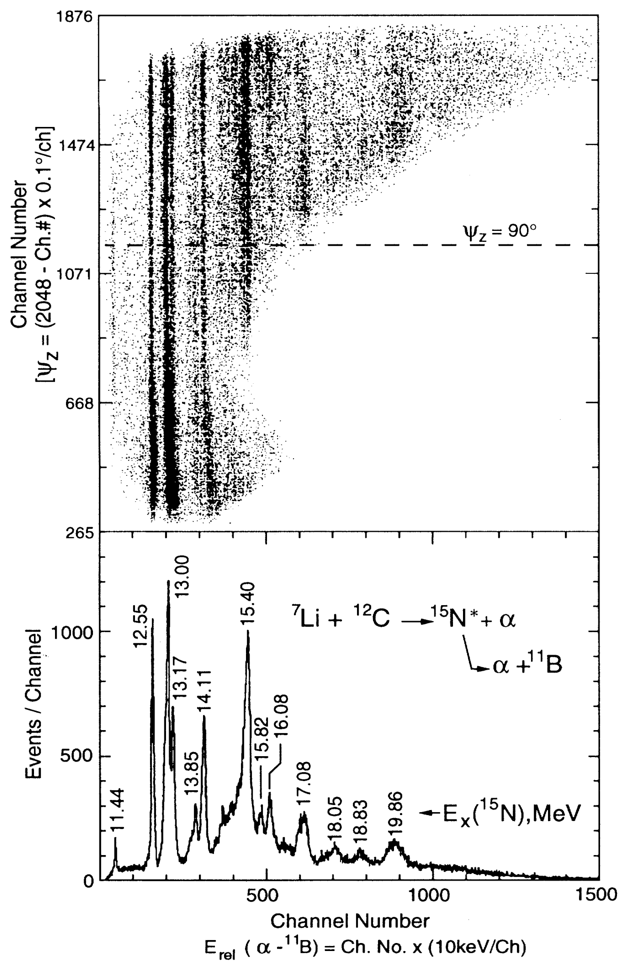

FIG. 3. Scatter plot of the $^{15}N^*$ decay energy (E_{rel}) on the horizontal axis vs the in-plane angle for the decay of $^{15}N^*(\psi_Z)$, and the projection of this scatter plot on the horizontal (E_{rel}) axis. Energy groups in this lower projection plot are labeled with the ^{15}N excitation energies in MeV. These events represent the total data acquired for the fixed detector geometry described in the text.

B. Alpha-particle decay angular correlations

Angular correlation data have been obtained for the six lowest energy states of Fig. 3. The alpha-particle yields for each of these states of ^{15}N are generated by spectrum fitting similar to that shown in Fig. 4(b). Those events are binned in the $\theta^*_{c.m.}$ vs Ψ_z plane in a 7° window about the emission angle, $\theta^*_{c.m.}$, and in a 10° interval in the $^{15}N^*$ decay angle, Ψ_z. The yields are corrected for coincidence detection efficiency by use of the Monte Carlo code BEAST (Ref. [7]), and then converted to double- differential cross sections. These angular correlations for the six prominent states below 14.2 MeV in excitation are displayed in Figs. 5 through 10. The range of the emission angle is chosen to maximize the decay angular range and

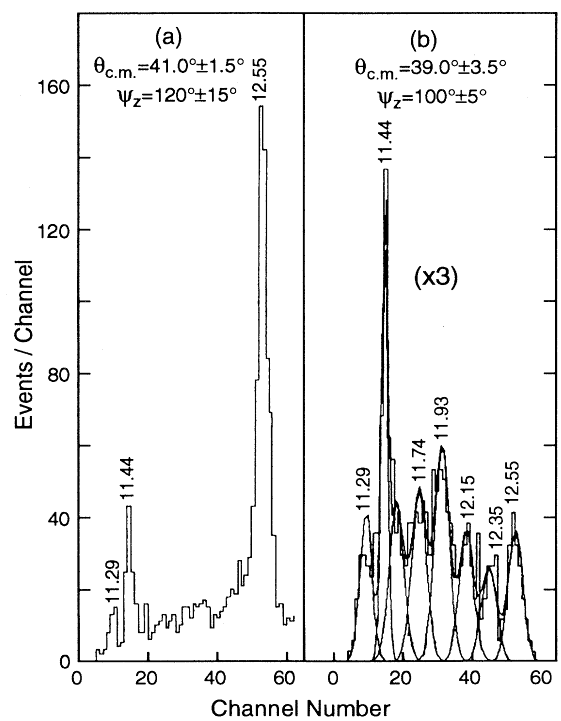

FIG. 4. Selected regions of decay angle phase space which illustrate improved energy resolution near the threshold for alpha-particle decay, E_{th}=10.99 MeV. $E_x(^{15}N)=E_{th}$ +Ch.No.×.03 MeV/ch.

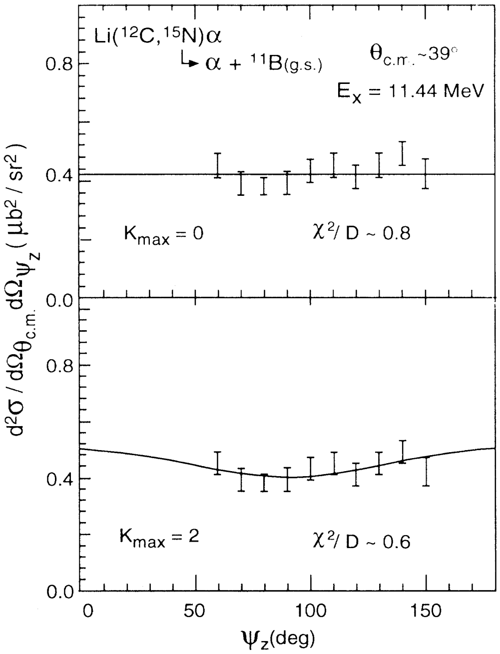

FIG. 5. Double-differential cross section for the alpha-particle decay of the intermediate state of ^{15}N* at an excitation energy of 11.44 MeV. Error bars represent statistical uncertainties only. Two representations of fitting by use of Eq. (2) are shown by the solid curves for two values of $K_{\max}$. The angles $\theta_{\text{c.m.}}$ and ψ_Z are defined in Fig. 1.

the statistical accuracy of the data. The immediately striking feature of these correlations is their remarkable symmetry about 90° relative to the beam axis, a result which is consistent with the PDDM assumption.

This general condition, the PDDM assumption, also yields isotropy in the azimuthal angle of this second binary decay [3]. The in-plane angular correlations, Figs. 5–10, can then be described by an even Legendre series as

$$\frac{d^2\sigma}{d\Omega\,(\theta^*_{\text{c.m.}})\;d\Omega(\psi_Z)} = \sum_{\substack{K=0,\\ \text{even}}}^{K_{\max}} a_K(\theta^*_{\text{c.m.}})\cdot P_K(\cos\psi_Z). \quad (2)$$

The maximum order of the series, $K_{\max}$, has been shown [3] to not exceed the minimum of $2J$ and $2\ell_2$, where J is the spin of the decaying state and ℓ_2 is the orbital angular momentum of the alpha-particle decay of the state. When a particular value of $K_{\max}$ provides a significantly better Legendre description of the data, then this value gives a lower limit for the J of the decaying state. For odd mass nuclides this is $J_{\min} = (K_{\max}+1)/2$. When two values of ℓ_2 exist for a given value of J^π, as is always the case in ^{15}N when $J \geq 3/2$, then the contribution to the cross section from the highest value of ℓ_2 is much smaller than the contribution from the lower value of ℓ_2 due to the large change in penetrability vs ℓ value near threshold. As a consequence, when the highest of the two values of ℓ_2 would have determined the value of $K_{\max}$ then the corresponding value of J^π is disfavored. Here those disfavored cases are for $J = J_{\min}$ and $\pi = (-1)^{K_{\max}/2}$.

For each measured angular correlation we determine by least squares fitting a $K_{\max}$ value and a set of coefficients $a_K(\theta^*_{\text{c.m.}})$. Due to the presumed azimuthal isotropy [3] and the integral properties of the Legendre functions, the branching fraction for decay by alpha-particle emission to the $^{11}\text{B}_{\text{g.s.}}$ is given by

$$\frac{\Gamma_{\alpha_0}}{\Gamma} = \left(\frac{4\pi a_0}{d\sigma/d\Omega_{\text{c.m.}}}\right). \quad (3)$$

Here $d\sigma/d\Omega$ is the ^{15}N* production cross section at the same c.m. reaction angle. Table I contains the essential measured quantities for each of the angular correlations, including the production cross sections [8]. The uncertainties quoted in Table I are statistical only. Absolute uncertainties in both the production and the decay cross sections are the order of 10%, so the branching fraction ratios have absolute uncertainties of about 15%. Branching fractions calculated by use of Eq. (3) are seen to be nearly independent of the $K_{\max}$ value chosen. The final values of $\langle\Gamma_{\alpha_0}/\Gamma\rangle$ (far right column of Table I) are based on the average of the two values corresponding to the two lowest values of χ^2/D for each E_x except for the state at

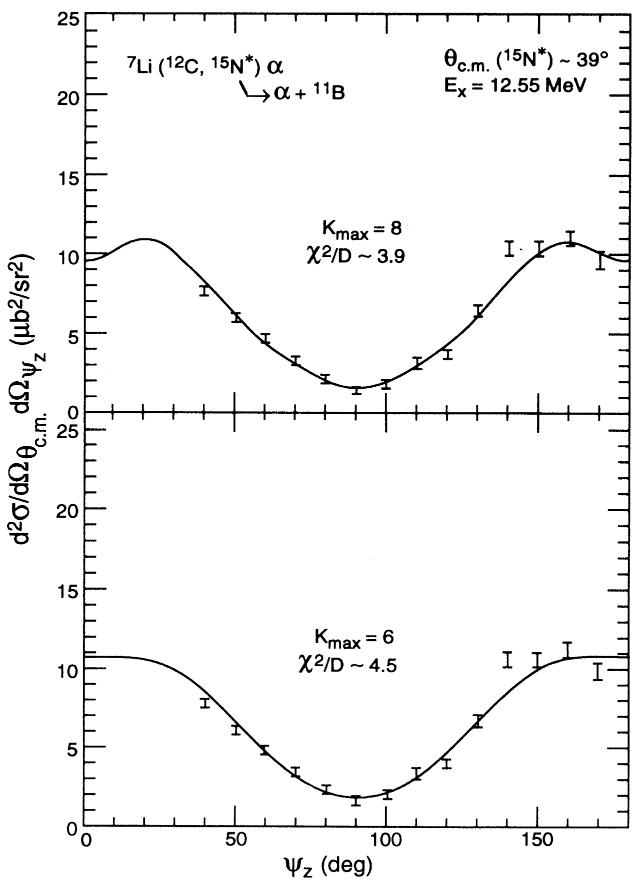

FIG. 6. Double-differential cross section for the alpha-particle decay of the intermediate state of ^{15}N* at an excitation energy of 12.55 MeV. See also caption of Fig. 5.

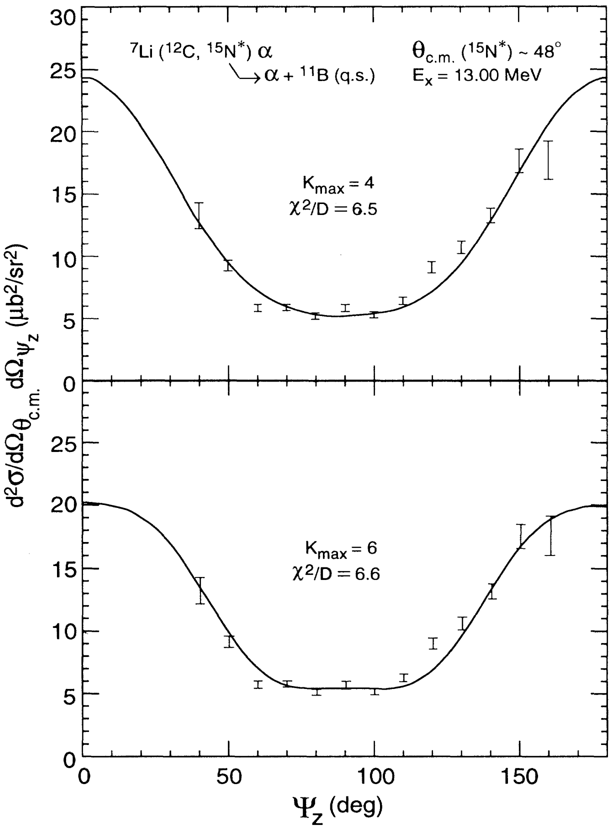

FIG. 7. Double-differential cross section for the alpha-particle decay of the intermediate state of $^{15}N^*$ at an excitation energy of 13.00 MeV. See also caption of Fig. 5.

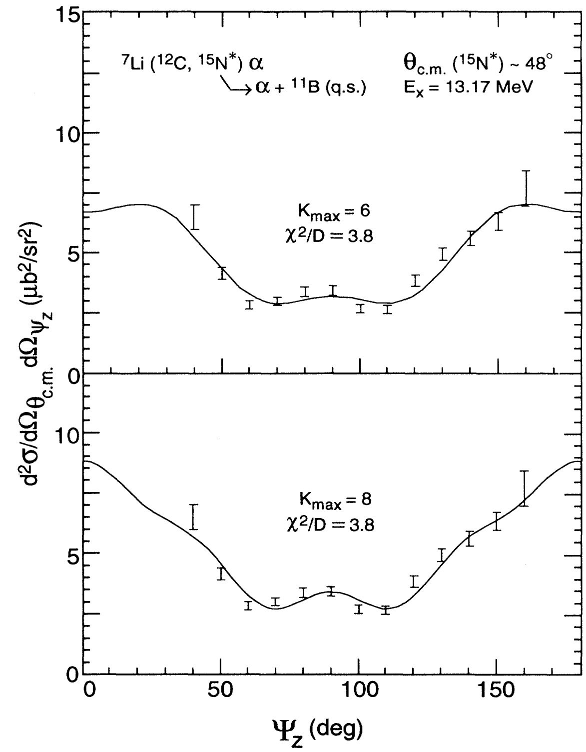

FIG. 8. Double-differential cross section for the alpha-particle decay of the intermediate state of $^{15}N^*$ at an excitation energy of 13.17 MeV. See also caption of Fig. 5.

E_x = 12.55 MeV where there are two independent data sets. The branching fractions for these six excited states in ^{15}N range from a threshold inhibited value of 6.8% for the E_x = 11.44 MeV state to an unusually high value of 84% for the state at E_x = 13.00 MeV. In all cases the statistical errors in the branching fractions are dominated by the errors in the production cross sections, and therefore they could be greatly reduced by a remeasurement of the cross sections for the two-body reaction $^{12}C + {}^7Li \rightarrow {}^{15}N^* + \alpha$.

There are two pieces of additional experimental evidence presented in these data which support the conclusion of azimuthal isotropy presented in Ref. [3]. First, the angular correlation for the decay of the state at E_x = 12.55 MeV (Fig. 6) is extracted at two different c.m. reaction angles with comparable decay angular range and statistical accuracy [3]. The resulting branching fractions are $\langle \Gamma_{\alpha_0}/\Gamma \rangle = 0.58\pm0.06$ for $\theta^*_{c.m.} \sim 39°$ and $\langle \Gamma_{\alpha_0}/\Gamma \rangle = 0.62\pm0.06$ for $\theta^*_{c.m.} \sim 48°$. The 15% absolute uncertainty does not apply to this comparison of values since the same targets were used for the two sets of measurements. The two branching fraction measurements for the 12.55 MeV state would not be expected to show such good agreement if the azimuthal correlations deviated significantly from isotropy. The second piece of evidence comes from the state at E_x = 11.44 MeV (see Fig. 5). For this state we

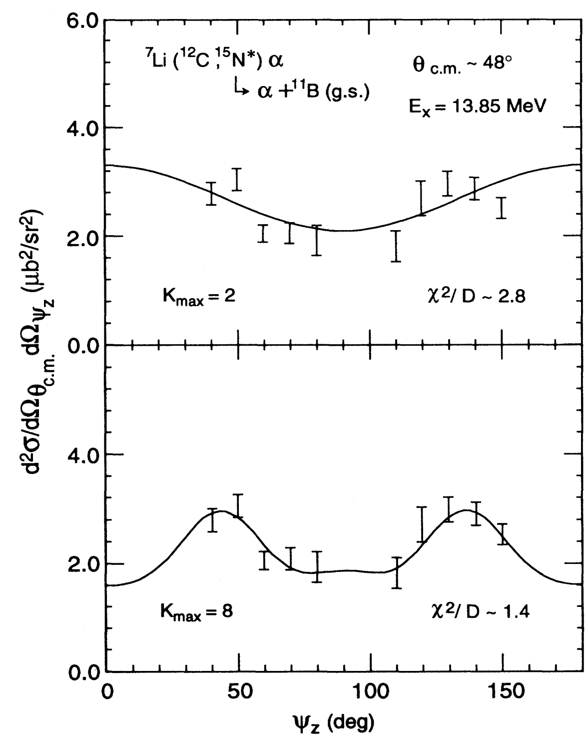

FIG. 9. Double-differential cross section for the alpha-particle decay of the intermediate state of $^{15}N^*$ at an excitation energy of 13.85 MeV. See also caption of Fig. 5.

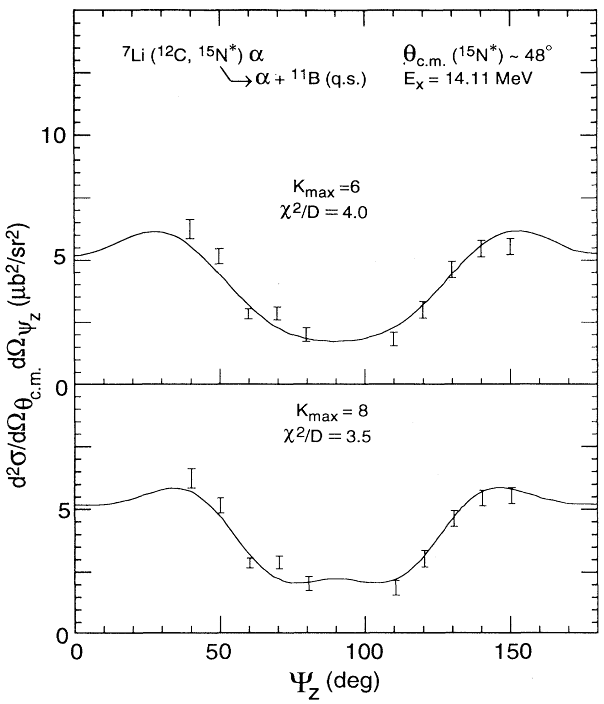

FIG. 10. Double-differential cross section for the alpha-particle decay of the intermediate state of $^{15}N^*$ at an excitation energy of 14.11 MeV. See also caption of Fig. 5.

measure a branching fraction of $\langle \Gamma_{\alpha_0}/\Gamma \rangle = 0.068\pm0.012$, including the 15% absolute uncertainty. Wang *et al.* [2] have studied this resonance directly and obtain a total width of 2.15±0.38 eV (see Table VI, Ref. [2]). Using their total width, our measurement yields an alpha-particle decay width $\Gamma_{\alpha_0} = (0.15\pm0.03)$ eV in good agreement with $\Gamma_{\alpha_0} = (0.11\pm0.03)$eV, which was obtained by Wang *et al.*.

C. Reduced widths, J^π values, and level widths

In Table II we display the information necessary for reduced width calculations for the states with previously known total widths, along with our results for reduced widths. The alpha-particle decay widths in Table II are the product of the total widths ($\Gamma_{\rm c.m.}$) of Table II and the branching fractions ($\langle \Gamma_\alpha/\Gamma \rangle$) of Table I but with the uncertainties in the branching fractions modified to include the 15% absolute uncertainty. The reduced widths listed in Table II are based on the assumption that the alpha-particle decay goes predominantly by the minimum allowed angular momentum and they are given by $\gamma^2_{\alpha\ell}=\frac{1}{2}\Gamma_\alpha/P_\ell$ [9]. Reasonable contributions from ℓ_2(max) will not greatly affect the results. The penetrabilities (P_{ℓ_2}) are interpolations from the tables of Thompson based on the work of Lane and Thomas [9,10].

The energy resolution in the vicinity of E_x-11.44 MeV is about 60 keV as shown in Fig. 4. There are two states here at nearly the same excitation energy, one with $J^\pi=\frac{1}{2}^+$ at 11.4351 MeV and one with $J^\pi=\frac{7}{2}^-$ at 11.4360 MeV [2]. Clearly the states are unresolvable in this experiment, however by width considerations it is unambiguous that we are observing predominantly the $\frac{7}{2}^-$ state. The Wigner limit for $^{15}N^*$ alpha-particle decay is about 470 keV when a channel radius of 5.5 fm is used. If we assume that our observation at 11.44 MeV represents the decay of the $\frac{1}{2}^+$ state, then the reduced width would be nearly 3 orders of magnitude greater than the Wigner limit, indicating that our data are overwhelmingly from the $\frac{7}{2}^-$ state and that the reduced width of this $\frac{7}{2}^-$ state is still nearly 25% of the Wigner limit. Any contribution of the $\frac{1}{2}^+$ state in the production cross section for our 11.44 MeV data would make the branching fraction for the $\frac{7}{2}^-$ state as calculated from Eq. (3) too small, therefore our value for the branching fraction for the $\frac{7}{2}^-$ state must be considered a lower limit. However, since our value is in good agreement with that of Wang *et al.* [2], the production cross section for the $\frac{1}{2}^+$ state must be much smaller than that of the $\frac{7}{2}^-$ state.

The state which we report at E_x=14.11 MeV could possibly be either of the states previously reported [1] with E_x=14.090 MeV and $J^\pi=(\frac{9}{2}^+,\frac{7}{2}^+)$ or with E_x=14.10 MeV and $J^\pi=\frac{3}{2}^+$. Unlike the comparison of possibilities at 11.44 MeV, the calculation of reduced widths does not distinguish between these choices in spite of the large spin difference. There is a slight preference for the high spin choice when considering the appropriate $K_{\rm max}$ values. The expected $K_{\rm max}$ would be ≤ 6 for the high spin state and ≤ 2 for the $J^\pi=\frac{3}{2}^+$ state. From the correlation fitting there is a slight preference for the higher $K_{\rm max}$ values (Table I), however, as can be seen in Fig. 10, poor statistical accuracy of the data makes a firm conclusion difficult on the basis of $K_{\rm max}$ values alone. There was insufficient data in the singles experiment for any meaningful FRDWBA comparison, however in the reaction $^{12}C(^7Li,\alpha)^{15}N^*$ this state at 14.11 MeV is seen to be comparatively weak at forward angles and much stronger at large angles, which is indicative of a high spin state. This is consistent with the fact that (^{7}Li,α) reactions usually preferentially populate high spin states. We conclude that the reduced width result is appropriately attributed to the state identified with $J^\pi=(\frac{9}{2}^+,\frac{7}{2}^+)$.

A state at E_x=14.11 MeV was previously reported [11] to have $J^\pi=\frac{13}{2}^+$ based on a compound nucleus analysis of the reaction $^{10}B(^7Li,d)^{15}N^*$ at (E^4Li)=24 MeV. This J^π value would require subsequent alpha-particle decay to proceed by ℓ=5 or 7. The small penetrability even for ℓ=5 leads to reduced widths of about one to four times the Wigner limit depending on the level widths listed (22 or 100 keV) in Table II. Although these reduced width values tend to disfavor such a large spin value for this state, it is important to point out that the same analysis [11] has yielded currently accepted high spin assignments for state at E_x=10.70 and 13.00 MeV, $J^\pi=\frac{9}{2}^+$ and $\frac{11}{2}^-$ respectively, while at the same time does not support the current $\frac{9}{2}^+$ assignment for the 12.56 MeV state.

The alpha-particle decay cross section for the ^{15}N state

TABLE I. Angular correlation parameters, production cross sections, and ground-state alpha-particle decay branching fractions for excited states of ^{15}N.

$E_x(^{15}\text{N})$ (MeV)	$\theta_{\text{c.m.}}$	$K_{\max}$ [a]	χ^2/D[a]	a_0[a] (μb/sr^2)	$d\sigma/d\Omega_{\theta_{\text{c.m.}}}$ [b] (μb/sr)	Γ_α/Γ	$\langle\Gamma_\alpha/\Gamma\rangle$[c]
11.44	39	0	0.8	0.42±0.01	78±7	0.068±0.006	0.068±0.006
		2	0.6	0.43±0.01		0.069±0.006	
12.55	39	2	5.8	5.35±0.09	115±11	0.58±0.06	
		4	4.9	5.28±0.09		0.58±0.06	
		6	4.5	5.34±0.09		0.58±0.06	
		8	3.9	5.34±0.09		0.58±0.06	0.60±0.04
	48	2	8.4	5.47±0.11	121±11	0.57±0.05	
		4	4.5	6.04±0.16		0.63±0.06	
		6	4.5	5.84±0.20		0.61±0.06	
		8	5.2	6.05±0.25		0.63±0.06	
13.00	48	2	9.0	9.00±0.15	144±15	0.79±0.08	
		4	6.5	9.65±0.18		0.84±0.09	
		6	6.6	9.60±0.20		0.84±0.09	
		8	8.1	9.08±0.23		0.79±0.08	0.84±0.09
13.17	48	2	7.3	4.04±0.08	156±20	0.33±0.04	
		4	5.1	4.28±0.09		0.34±0.05	
		6	3.8	4.22±0.10		0.34±0.04	
		8	3.8	4.27±0.11		0.34±0.05	0.34±0.04
13.85	48	2	2.8	2.41±0.07	75±18	0.40±0.10	
		4	1.7	2.24±0.10		0.38±0.09	
		6	1.7	2.20±0.10		0.37±0.09	
		8	1.4	2.23±0.23		0.37±0.10	0.37±0.09
14.11	48	2	4.3	3.75±0.09	147±29	0.32±0.06	
		4	4.5	3.60±0.13		0.31±0.06	
		6	4.0	3.63±0.14		0.31±0.06	
		8	3.5	3.63±0.31		0.31±0.07	0.31±0.06

[a]Angular correlation parameters from fitting by use of Eqs. (2) and (3).
[b]Production cross sections for ^{15}N*, in the reaction ^{12}C+^{7}Li→ α+^{15}N*, at E_x and $\theta_{\text{c.m.}}$ values given.
[c]Average values of branching fractions in the previous column for the two lowest values of χ^2/D at each E_x. Statistical uncertainty is reduced for the E_x=12.55 MeV value since the average involves two independent data sets. See Ref. [3].

at E_x=13.85 MeV is the smallest of the angular correlations measured, but it also shows the most angular structure. Although the statistical accuracy is not good, the data show a clear preference for a large value of $K_{\max}$ rather than $K_{\max}$=2 which is expected on the basis of the currently accepted J^π value of $\frac{3}{2}^+$. A description of the data with $K_{\max}$ >2 would necessitate a J^π assignment of $\frac{5}{2}^-$ or $\geq \frac{7}{2}^\pm$. Even with the minimum J^π values consistent with $K_{\max}$=6, the reduced widths would still be less than 50 keV.

The ^{15}N excited state at E_x=13.17 MeV has a suggested [1] spin of J=($\frac{9}{2}$) and our value of $K_{\max}$ is consistent with that. However, recent polarized beam work [12] on the reaction, ^{12}C($^6\vec{\text{Li}}$,^{3}He) which excites many of these same states in ^{15}N, has confirmed the $\frac{9}{2}^+$ assignments for the states at 10.69 and 12.55 MeV, while ruling out $J^\pi=\frac{9}{2}^+$ or $\frac{9}{2}^-$ for the 13.17 MeV state. Their work indicates $J^\pi=\frac{7}{2}^+$ or $\frac{5}{2}^-$ for this state. The expected $K_{\max}$ value for the alpha-decay angular correlation would be 6 for $J^\pi=\frac{7}{2}^+$ or $\frac{9}{2}^+$, but would be 8 for $\frac{9}{2}^-$ and only 4 for $\frac{5}{2}^-$. Since the angular correlation shows a preference for a $K_{\max}$ of 6 or 8, the combined results of our work and that of Kemper *et al.* [12] would favor an assignment of $J^\pi=\frac{7}{2}^+$ for the 13.17 MeV state, in agreement with the earlier conclusion of van der Borg *et al.* [13].

Angular correlations have also been measured for the two excited states at E_x=12.55 and 13.00 MeV. These states have well-established values of $J^\pi=\frac{9}{2}^+$ and $\frac{11}{2}^-$, respectively, however their natural widths are unknown. Although these states have the largest branching fractions of any of the alpha-particle decays which we have measured, we are unable to evaluate the reduced widths. The single-particle width for alpha particles can be evaluated from the penetrabilities and the Wigner limit for alpha-particle reduced width as $\Gamma_\alpha^{\text{SP}}=2\times P_\ell \times \Gamma_\alpha^{\text{WL}}$. One would expect the actual alpha-particle reduced widths to

TABLE II. Partial widths and reduced widths for the ground-state alpha-particle decay of states in ^{15}N with known J^π and total width.

Correlation	Previous information			Deduced width information			
E_x (MeV)	E_x (MeV)[a]	J^π [a]	$\Gamma_{c.m.}$[a]	Γ_{α_0}[b]	ℓ_2	$P_{\ell_2(\min)}$	$\gamma^2_{\ell_2(\min)}$
11.44	11.4351	$\frac{1}{2}^+$	38.2±4 keV	2.6±0.5 keV[c]	1	$4.4(10)^{-6}$	$3(10)^5$ keV[c]
	11.4360	$\frac{7}{2}^-$	2.15±0.38 eV	0.15±0.03 eV	2,4	$6.9(10)^{-7}$	110±20 keV
13.17	13.174	$(\frac{9}{2})$	7±3 keV	2.4±1.0 keV	3,5	$8.4(10)^{-2}$	14±6 keV
13.85	13.84	$\frac{3}{2}^+$	75 keV	28±8 keV	1,3	1.3	11±3 keV
14.11	14.090	$(\frac{9}{2}^+, \frac{7}{2}^+)$	22±6 keV	6.8±2.5 keV	3,5	0.43	8±3 keV[c]
	14.10	$\frac{3}{2}^+$	~100 keV	(~31±8 keV)	1,3	1.5	(10±3 keV)

[a]From Ref. [1] except for the 11.44 MeV doublet for which Tables I and VI of Ref. [2] are used.
[b]From $\langle\Gamma_\alpha/\Gamma\rangle$ of Table I including 15% absolute error, and from the previous column of this table.
[c]Our decay correlation cannot be predominantly through the $\frac{1}{2}^+$ state since the resulting reduced width would then exceed the Wigner limit (~470 keV) by nearly $\times(10)^3$. A similar exclusion cannot be made for the 14.11 MeV doublet however excitation of the high spin state is favored.

be less than the Wigner limit. Corresponding approximate limits on the total widths would be just the quotient of the single-particle widths and the branching fractions. These values and the parameters necessary for their calculation are summarized in Table III. The total widths approximated by this method are $\leq$1 keV for the state at E_x=12.55 MeV and $\leq$8 keV for the state at 13.00 MeV. Actual upper limits may be as much as a factor of three times as large as these values due to the number of ways an alpha particle can be formed from the nucleons available in ^{15}N and ^{11}B. As before the penetrabilities used correspond to the lowest allowed value of ℓ_2. The observed values of $K_{\max}$ for the correlations through these two states are consistent with the requirement that $K_{\max}$ be less than or equal to the minimum of $2J$ and $2\ell_2$. Planned future experiments will attempt to place width limits on these states by direct measurement rather than by the assumptions discussed herein. Improved energy resolution is particularly important in this energy region since there may be as many as four states within a few hundred keV [1], which in the present experiment leads to difficulties in accurately extracting the decay yield.

IV. CONCLUSION

Branching fractions for alpha-particle decay, $^{15}\mathrm{N}^* \to \alpha + ^{11}\mathrm{B}_{\mathrm{g.s.}}$, have been measured for ^{15}N states at excitation energies of 11.44, 12.55, 13.00, 13.17, 13.85, and 14.11 MeV, demonstrating that the method of resonant particle decay spectroscopy (RPDS) is a very effective tool for obtaining this information. For ^{15}N excited states with known level width (E_x=11.44, 13.17, 13.85, and 14.11 MeV) we have extracted the α_0-partial decay widths and the reduced widths for the assumption that the decay proceeds by the minimum allowed angular momentum. Good agreement is achieved for the one previously known value for the 11.44 MeV, $\frac{7}{2}^-$ state, which had been determined by direct resonance measurement. It is shown that our data at E_x=11.44 MeV are predominantly from the alpha-particle decay of the $\frac{7}{2}^-$ state rather than from the unresolved $\frac{1}{2}^+$ state, since the latter interpretation would yield a reduced width exceeding the Wigner limit by nearly a factor of 10^3.

The order of the Legendre expression for the correla-

TABLE III. Width estimates for states of ^{15}N at E_x=12.55 and 13.00 MeV.

E_x (MeV)	J^π	$\langle\Gamma_{\alpha_0}/\Gamma\rangle$[a]	Allowed ℓ_2	P_{ℓ_0}[b]	Γ_{α_0}[c]	Γ[d]
12.55	$\frac{9}{2}^+$	0.60±0.10	3,5	$7.4(10)^{-4}$	$\lesssim$0.7 keV	$\lesssim$1 keV
13.00	$\frac{11}{2}^-$	0.84±0.15	4,6	$7.4(10)^{-3}$	$\lesssim$7 keV	$\lesssim$8 keV

[a]Values from Table I modified to include the 15% absolute error.
[b]Penetrability interpolated from the tables of Thompson (Ref. [10]) for the minimum allowed value of ℓ_2.
[c]Estimated value of alpha-particle partial width assuming that the reduced width is $\lesssim$ the Wigner limit (470 keV). $\Gamma_\alpha \lesssim 2\, P_\ell \cdot \Gamma_{\mathrm{WL}}$.
[d]Estimated total widths from partial widths of previous column and the measured branching fractions. $\Gamma_{\mathrm{total}} = \Gamma\alpha / \langle\Gamma_\alpha/\Gamma\rangle$. Actual upper limits on widths could be as much as three times as large.

tion through the state at 13.17 MeV, together with the recent polarization measurements by Kemper *et al.*, favors a J^π assignment of $\frac{7}{2}^+$ rather than the suggested $J = (\frac{9}{2})$ listed in the current ^{15}N compilation. For the correlation through the 14.11 MeV state, where there also exists a doublet, the Wigner limit argument disfavors but does not forbid a possible $J^\pi=\frac{13}{2}^+$ assignment, and the order of the Legendre description of the correlation data favors the excitation of the state with tabulated $J^\pi=(\frac{9}{2}^+,\frac{7}{2}^+)$. The RPDS method has also been used to obtain level width estimates for the states at E_x=12.55 and 13.00 MeV, which are found to be very narrow.

We wish to emphasize that the symmetry about ψ_Z=90° for values of $\theta_{\rm c.m.}$ which are intermediate between 0° and 90°, which we have observed in the double-differential cross sections, is a very unique and totally unexpected feature. The explanation of this symmetry in terms of the PDDM assumption [3] implies in addition that the azimuthal correlation will be isotropic. The accuracy of the branching fractions and reduced widths presented in this work rely on this implication. If an alternative and satisfactory explanation of the symmetry about ψ_Z=90° can be found, then the interpretations in the present work may be invalid, until the azimuthal correlations can be measured so that proper integrations of the full correlation function can be made. Alternatively, if azimuthal correlations were to show isotropy for the cases of symmetry about ψ_Z=90°, then the implications of Ref. [3] would be directly validated. In the ^{15}N* $\rightarrow \alpha+^{11}$B$_{\rm g.s.}$ work there are three experimental features which are consistent with or yield consistent results by use of the PDDM assumption. (1) The in-plane correlations are symmetric about Ψ_Z=90°. (2) We obtain the same branching fraction for ^{15}N* $\rightarrow \alpha+^{11}$B$_{\rm g.s.}$, E_x = 12.55 MeV, at two different values of $\theta^*_{\rm c.m.}$. (3) We obtain a partial width for the alpha-particle decay of the 11.436 MeV, $\frac{7}{2}^-$ state which agrees with the directly measured result of Ref. [2]. The difficult measurements of azimuthal correlations for the particle decay of excited states near the decay threshold are currently under development in this laboratory.

ACKNOWLEDGMENTS

The authors wish to acknowledge the many helpful discussions concerning this work with Dr. D. Robson and Dr. K.W. Kemper and the technical assistance of Dr. A.D. Frawley and Dr. E. Myers. This work was supported in part by the National Science Foundation Grant PHY-9210082.

[1] F. Ajzenberg-Selove, Nucl. Phys. **A523**, 1 (1991).
[2] T.R. Wang, R.B. Vogelaar, and R.W. Kavanagh, Phys. Rev. C **43**, 83 (1991).
[3] J.A. Liendo, N.R. Fletcher, and D. Robson, Phys. Rev. C **47**, 682 (1993).
[4] W.D.M. Rae and R.K. Bhowmik, Nucl. Phys. **A420**, 320 (1984); R.K. Bhowmik and W.D.M. Rae, Phys. Lett. **136B**, 149 (1984); S. March and W.D.M. Rae, *ibid.* **153B**, 21 (1985).
[5] W.D.M. Rae, A.J. Cole, A. Dacal, R. Legrain, B.G. Harvey, J. Mahoney, M.J. Murphy, R.G. Stokstad, and I. Tserruya, Phys. Lett. **105B**, 417 (1981); W.D.M. Rae, A.J. Cole, B.G. Harvey, and R.G. Stokstad, Phys. Rev. C **30**, 158 (1984).
[6] D.D. Caussyn, G.L. Gentry, J.A. Liendo, and N.R. Fletcher, Phys. Rev. C **43**, 205 (1991).
[7] D.D. Caussyn, Ph.D. dissertation, Florida State University, 1990, unpublished.
[8] J.A. Liendo, Ph.D. dissertation, Florida State University, 1993, unpublished.
[9] A.M. Lane and R.G. Thomas, Rev. Mod. Phys. **30**, 257 (1958).
[10] W.J. Thompson, Florida State University internal report, 1965, unpublished.
[11] W. Kohler, H. Schmidt-Böcking, and K. Bethge, Nucl. Phys. **A262**, 113 (1976).
[12] K.W. Kemper, P.L. Kerr, A.J. Mendez, E.G. Myers, E.L. Reber, K. Rusek, and G. Tungate, Phys. Lett. B **321**, 183 (1994).
[13] K. van der Borg, R.J. de Meijer, A. van der Woude, and H.T. Fortune, Phys. Lett. **84B**, 51 (1979).